Environmental Science and Pollution Research (2020) 27:33–42
https://doi.org/10.1007/s11356-019-06474-3

CURRENT TRENDS ON SUSTAINABLE ENERGY, ENGINEERING, MATERIALS AND ENVIRONMENT

The impact of hot metal temperature on CO_2 emissions from basic oxygen converter

José Díaz[1] · Francisco Javier Fernández[1]

Received: 27 January 2019 / Accepted: 9 September 2019 / Published online: 14 September 2019

Abstract

Recycled steel is a key material for sustainable development. However, not all steel demand can be met by recycling, and therefore, new metallic iron must be introduced in the global cycle. The transformation of iron oxides into steel requires carbon which is oxidized into CO_2. This paper focuses on the basic oxygen furnace (BOF) where molten iron is converted into liquid steel. In order to assess the effect of molten iron temperature on CO_2 emissions, the process has been modelled using mass and energy balances. Model results show that, for a typical converter charge, a slight increase of 10 °C can lead to a direct reduction of 0.006 t of CO_2 per ton of liquid steel. A total variation of 0.17 t of CO_2 per ton of liquid steel is found depending on plant strategy and process constraints. Finally, different actuation levers for carbon mitigation are assessed. It can be concluded that operation and modelling improvements should be jointly addressed to exploit their full potential for carbon footprint reduction.

Keywords Steelmaking · BOF converter · Carbon footprint · Mass balance · Energy balance · Emission assessment · Fundamental mechanistic modelling

Introduction

Steel is on the road to be a major player for sustainable development and circular economy (Worldsteel 2018). It can be produced at an integrated facility from iron ore or at a secondary facility, mainly from recycled steel scrap. As shown in Fig. 1, an integrated site typically includes coke ovens (CO), sinter plants (SP), blast furnaces (BF), and basic oxygen furnaces (BOF). Sinter plants prepare iron oxides for the blast furnaces while coke ovens transform coal into coke which is fuel and reducing agent for the blast furnace. By contrast, secondary steelmaking produces steel by melting scrap in the electric arc furnaces (EAF).

From an economic global point of view, it is always more convenient to recycle steel than to mine iron ore. The same conclusion is met when considering energy, natural resources, or emissions. However, several issues, as limited scrap availability or the lower quality of EAF steels, have made BOF the prevailing route with more than 70% of world steel production (Worldsteel 2019). Since not all steel demand can be met by recycling, new metallic iron must be introduced in the global cycle through integrated steelmaking, as has been reviewed by Yellishetty et al. (2011).

The transformation of iron oxides into steel makes use of huge amounts of reducing agents, being carbon the most important. This produces a substantial volume of carbon dioxide and, consequently, the environmental conscious steelmaker must be well aware about how his process is affecting CO_2 emissions.

There is a number of relevant studies on carbon footprint for the steelmaking industry (Ryman and Larsson 2006; Barati 2010). These works are essential to understand the behavior of the integrated mill and to ensure that improvements in a part of the process do not affect adversely the entire facility. However, these analyses tend to rely on very simple fixed sub-processes models, not allowing BOF engineers to identify or assess local improvements.

On the contrary, hot metal management at BOF plant level has received a lot of attention regarding energy, productivity, and cost optimization (Ares et al. 2010) but little information has been published on how it is affecting the carbon total emissions. In a previous study, temperature was identified as

Responsible editor: Philippe Garrigues

✉ José Díaz
diazjose@uniovi.es

[1] Polytechnic School of Engineering, University of Oviedo, 33204 Gijón, Spain

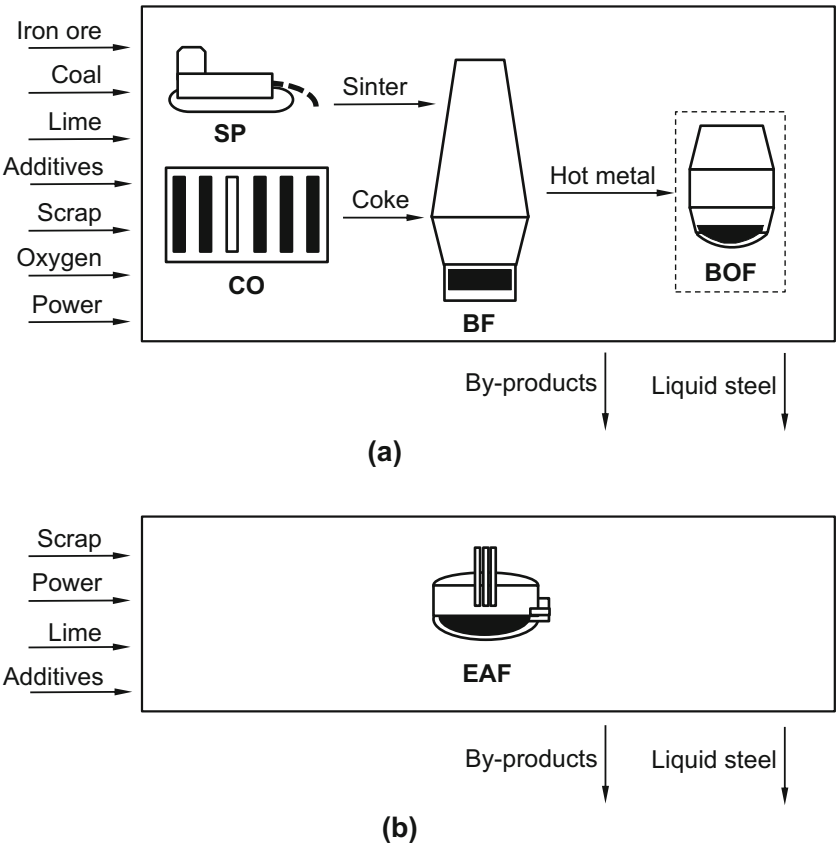

Fig. 1 Main routes for liquid steel production: **a** integrated facility with sinterplants (SP), coke ovens (CO), blast furnaces (BF), and basic oxygen furnaces (BOF); **b** secondary facility with electric arc furnaces (EAF)

an important lever for hot metal consumption optimization (Díaz et al. 2018), while this present work analyzes the impact of hot metal temperature on direct and indirect carbon emissions.

In the BOF process, depicted in Fig. 2, a carbon-rich molten iron, the hot metal, coming from the blast furnace, is transformed into liquid steel by blowing oxygen and making use of steel scrap, inert gases like nitrogen or argon, and other additives as lime, iron ore, or anthracite. A complete overview of BOF process is provided by Miller et al. (1998). It is a

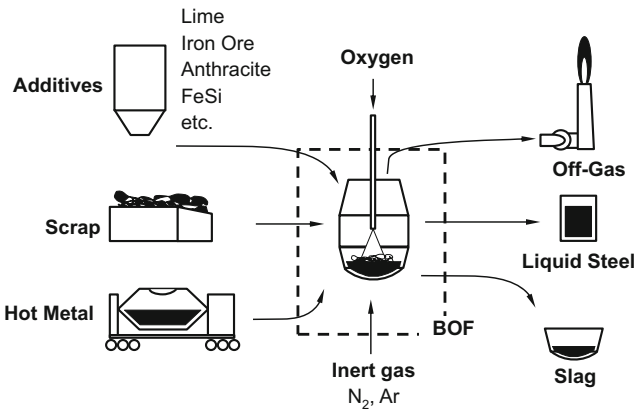

Fig. 2 Schematic representation of BOF system with input and output materials

discontinuous process in which each batch is often referred as "a heat" and produces typically 200 to 300 t of liquid steel. Oxidation conditions inside the BOF not only remove impurities as C, Si, or P from hot metal but also provide energy for heating and melting the scrap and rising the temperature of the melt from initial conditions of around 1200 °C up to final steel target above 1600 °C. Oxidation products as SiO_2 or P_2O_5 are assimilated by lime and other flux additives into the slag phase, while C is oxidized to CO and CO_2 carried out in off-gas phase.

In normal production, a target steel is set in terms of mass, chemistry, and temperature while the required amounts of hot metal, scrap, oxygen, and other additives are determined by a process control model. For a given target steel, hot metal to scrap ratio strongly depends on hot metal temperature and chemistry. However, by using suitable exo- or endothermic additives, a wide range of hot metal ratios can satisfy both mass and energy balances. Hence, the optimum hot metal ratio, in terms of cost, quality, productivity, or other considerations, can be found. Consequently, hot metal strategy should be always taken into account.

In this study, a general mathematical model for quantifying carbon emissions from BOF converter is presented. The model is extensively validated against real plant results for two different converters along a year. Subsequently, the validated model is applied to 160 study cases, covering four different

hot metal strategies and a temperature range from 1200 to 1300 °C. Target steel and hot metal chemistry were kept constant while the required amounts of hot metal, scrap, oxygen, iron ore, anthracite, and FeSi were calculated by the model, together with slag and off-gas volumes and compositions. In the light of model results, the role of actual process conditions and future developments on carbon footprint are analyzed.

System modelling

In order to draw meaningful conclusions, a model based on mass and energy balances has been developed. It is well known that such a macroscopic and mechanistic approach generalizes well (Mazumdar and Evans 2010), being the best option for application in different plants and under diverse production scenarios.

Since mass and energy balances depend on the degree of oxidation of the involved chemical species, which in turn depends on the quantity of oxygen blown into the BOF, both balances are coupled and must be simultaneously satisfied.

Mass balance

Mass conservation applied to a steel batch implies that the total mass of loaded materials (hot metal, scrap, additives, oxygen, inert gasses) equals total mass of obtained products (liquid steel) and by-products (slag and off-gas). Moreover, mass balance must be separately satisfied for different chemical species involved in the process:

$$m_{st}x_{st}^{j} + m_{sl}x_{sl}^{j} + m_{OG}x_{OG}^{j} = m_{HM}x_{HM}^{j} + m_{sc}x_{sc}^{j} + m_{ad}x_{ad}^{j} + m_{O_2}x_{O_2}^{j} + m_{IG}x_{IG}^{j} \quad (1)$$

where m_i and x_i^j represent the total mass and mass fraction of species j for each material i. The subscripts st, sl, OG, HM, sc, ad, O_2, and IG indicate steel, slag, off-gas, hot metal, scrap, additives, oxygen, and inert gases, respectively.

Since the mass and the chemistry of target steel are fixed while gaseous oxygen input must be calculated, it is convenient to express Eq. (1) in the form:

$$m_{st} + m_{sl} + m_{OG} = m_{in}^{O} + \sum_{i\in input}\left(1-x_i^{O}\right)m_i \quad (2)$$

where the total oxygen input, $m^o{}_{in}$, comprises not only gaseous oxygen but also atomic oxygen coming from input materials, as iron oxide from iron ore, that are reduced providing further oxygen to the process.

Equation (1) can also be expressed as:

$$m_{st}x_{st}^{j} + m_{sl}x_{sl}^{j} + m_{OG}x_{OG}^{j} = m_{in}^{j} \quad (3)$$

where m_{in}^{j} represents the total input mass of species j. Oxygen is present in the oxides of slag and off-gas phases, but also in the liquid steel as atomic dissolved oxygen. Hence, Equation (3) can be written for oxygen as:

$$m_{st}x_{st}^{O} + m_{sl}x_{sl}^{O} + m_{OG}x_{OG}^{O} = m_{in}^{O} \quad (4)$$

Other elements as Fe, Si, Mn, and P are partially oxidized to slag phase while the rest will remain in the steel melt:

$$m_{st}x_{st}^{Fe} + m_{sl}x_{sl}^{Fe} = m_{in}^{Fe} \quad (5)$$

$$m_{st}x_{st}^{Si} + m_{sl}x_{sl}^{Si} = m_{in}^{Si} \quad (6)$$

$$m_{st}x_{st}^{Mn} + m_{sl}x_{sl}^{Mn} = m_{in}^{Mn} \quad (7)$$

$$m_{st}x_{st}^{P} + m_{sl}x_{sl}^{P} = m_{in}^{P} \quad (8)$$

Carbon is only partially removed from the metal in the form of gaseous oxides while carbon content in the slag can be neglected:

$$m_{st}x_{st}^{C} + m_{OG}x_{OG}^{C} = m_{in}^{C} \quad (9)$$

Oxide inputs from fluxes (lime, dolomitic lime, or gravel) are better considered as a single species since they do not experience further oxidation upon incorporation to slag phase:

$$m_{sl}x_{sl}^{CaO} = m_{in}^{CaO} \quad (10)$$

$$m_{sl}x_{sl}^{MgO} = m_{in}^{MgO} \quad (11)$$

$$m_{sl}x_{sl}^{SiO_2} = m_{in}^{SiO_2} \quad (12)$$

Inert gases escape with off-gas phase after providing melt agitation. Some nitrogen remains dissolved in steel but argon solubility can be neglected.

$$m_{st}x_{st}^{N_2} + m_{OG}x_{OG}^{N_2} = m_{in}^{N_2} \quad (13)$$

$$m_{OG}x_{OG}^{Ar} = m_{in}^{Ar} \quad (14)$$

Two additional independent equations can be posed by taking into account that the sum of mass fractions in gas and slag phases equals 1:

$$\sum_{j\in sl}x_{sl}^{j} = 1 \quad (15)$$

$$\sum_{j\in OG}x_{OG}^{j} = 1 \quad (16)$$

Finally, the stoichiometric relations for off-gas and slag oxides allow to express oxygen content as a function of other element contents:

$$x_{sl}^{O} = x_{sl}^{Si}\frac{32}{28} + x_{sl}^{Mn}\frac{16}{55} + x_{sl}^{P}\frac{80}{62} + x_{sl}^{Fe}k_{Fe} \quad (17)$$

$$x_{OG}^{O} = x_{OG}^{C}(1+k_{PC})\frac{16}{12} \quad (18)$$

Table 1 Average and standard deviation (in parentheses) of measured temperature and chemical composition for hot metal and steel

	T (°C)	C (% mass)	Si (% mass)	Mn (% mass)	P (% mass)	O (% mass)
Hot metal	1334 (56)	4.6 (0.21)	0.40 (0.11)	0.29 (0.05)	0.07 (0.006)	
Steel	1689 (67)	0.035 (0.01)	0.002 (0.002)	0.096 (0.022)	0.011 (0.004)	0.075 (0.015)

where the constants k_{Fe} and k_{PC} take into account the rate of different oxidation products for iron (FeO/Fe_2O_3) and carbon (CO/CO_2), respectively.

Energy balance

Energy conservation for a steel batch leads to

$$\sum_{i\in input} m_i h_i = \sum_{i\in output} m_i h_i + Q_{TL} \tag{19}$$

where h_i is the specific enthalpy of material i and Q_{TL} accounts for furnace thermal losses. Since reaction enthalpies at standard metallurgical conditions of 1600 °C and 1 atm are available in literature (Kudrin 1985; Ghosh and Chatterjee 2008), Equation (19) can be expressed in a more convenient way by

$$\sum_{i\in output} m_i \Delta h_{M-Fi} - \sum_{i\in input} m_i \, \Delta h_{M-Ii} + \Delta H_r^M + Q_{TL} = 0 \tag{20}$$

where $-\Delta h_{M-Ii}$ represents the enthalpy variation, including decomposition, heating, and dissolution, of the raw material i from initial to metallurgical conditions while Δh_{M-Fi} is the enthalpy variation of product i from metallurgical to final conditions. The enthalpy difference between inputs and outputs at their respective conditions is due to reaction enthalpies, ΔH_r^M, and thermal losses.

Model validation

The set formed by Eqs. (2), (4–18), and (20) can be analytically or numerically solved. For the goal of this research, the numerical approach is chosen since it is straightforward and computing time is not a critical issue. Material properties and transformation-reaction enthalpies are taken from data available in the literature (Miller et al. 1998; Kudrin 1985; Ghosh and Chatterjee 2008) which are in good agreement with plant practices and process models (Yawata 1986). Moreover, usual assumptions were adopted for equation solving as fixed iron content in slag (18%, see Table 4), constant thermal losses (5%), final slag temperature equal to final steel temperature, average off-gas temperature equal to average melt temperature, carbon oxidation to CO/CO_2 (90/10%) in the reaction site and then totally to CO_2, and $Fe^{3+}/(Fe^{3+}+Fe^{2+}) = 0.3$.

Model validation was performed against real plant results for a dataset composed of 760 heats, encompassing two different converters along a full production year with different hot metal scenarios. As can be seen from input variables in Tables 1 and 2, a reasonably wide domain was covered by validation tests.

Model performance in terms of energy imbalance is displayed in Fig. 3 where individual energy prediction error is always below 4% while moving average of errors is below 1.5% when considering a typical production of 21 heats per day. Similarly, oxygen prediction error is always less than 8% for individual heats and less than 5% for daily averages. Finally, steel mass prediction error is lower than 6% for individual heats and below 3% for daily averages. Individual errors can be not very representative as can be adversely influenced by occasional measurement errors. Particularly, mass measurements can also be affected by operative issues, since a small but unknown amount of steel can be poured with slag.

Although existing statistical models for on-line process control could provide more accurate short-term predictions, their better performance tends to rely on continuous feedback from process results as pointed out by Sickert and Schramm (2007). By contrast, the proposed model exhibits stable accuracy without additional corrections, making it a valid tool for analyzing the behavior of the process under very diverse, even hypothetical, production scenarios.

Cases of study

CO_2 emissions were calculated for hot metal temperatures between 1200 and 1300 °C under the four plant strategies that

Table 2 Mean and standard deviation (in parentheses) of input masses in tons

Hot metal	Scrap	Lime	Dolo. lime	Iron ore	Anthracite	FeSi	N_2	Ar	O_2
251 (14)	62 (11)	14 (2.3)	1.1 (2.0)	0.6 (1.2)	1.4 (1.7)	0.11 (0.28)	0.06 (0.06)	0.11 (0.11)	23.0 (2.2)

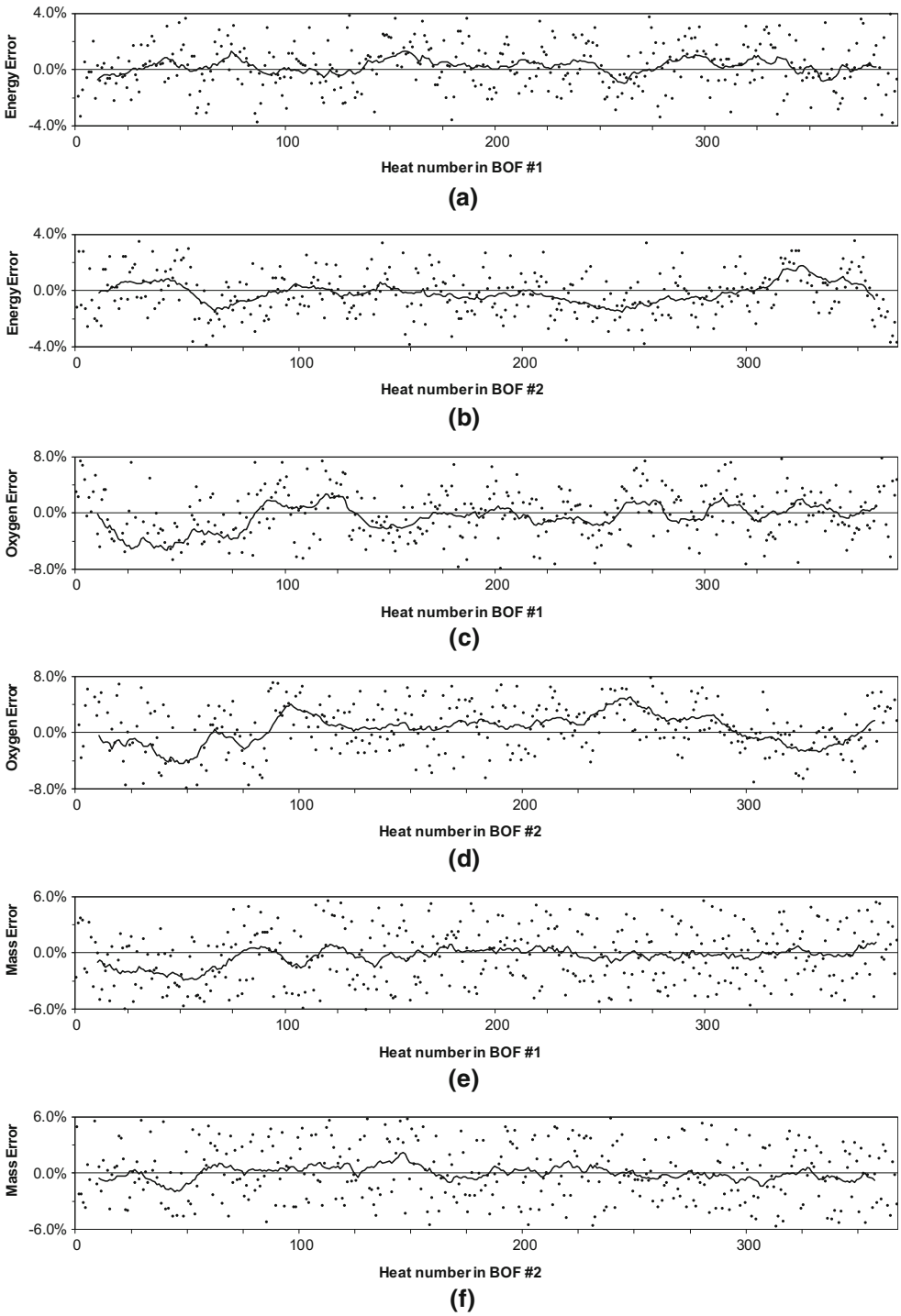

Fig. 3 Evolution of model balance errors along a year: **a** energy in BOF #1; **b** energy in BOF #2; **c** oxygen in BOF #1; **d** oxygen in BOF #2; **e** mass in BOF #1; and **f** mass in BOF #2; each dot represents a single heat and the solid line represents the two-sided moving average for a window of 21 heats

can be adopted by process engineers, depending on market or production circumstances:

(a) Neutral energy balance, just with hot metal and scrap, without cooling or heating additives.
(b) Maximized hot metal, using iron ore pellets as coolant.
(c) Minimized hot metal, using anthracite as heating additive.
(d) Minimized hot metal, using FeSi as heating additive.

Representative quantities and chemistries for input materials and production targets were adopted as given in Tables 3 and 4, respectively. Direct emissions from BOF were obtained directly from the model output while indirect emissions were taken from Ryman and Larsson (2006) and are shown in Table 5. Since there are certain operating limits for

Table 3 Mass, temperature, and composition of input materials

Material	*m* (t)	*T* (°C)	Chemical composition (% mass)									
			Fe	C	Si	Mn	P	O	N	Ar	CaO	MgO
Hot metal	m	v	94.39	4.80	0.46	0.27	0.08					
Scrap	m	25	99.42	0.05	0.01	0.50	0.02					
Lime	15	25									95	5
Dol. lime	5	25									63	37
Iron ore	v	25	70					30				
Anthracite	v	25		100								
FeSi	v	25	25		75							
N_2	0.15	25							100			
Ar	0.25	25								100		
O_2	m	25						100				

v, variable of the study; *m*, model result

the different input materials, the imposed constraints are indicated in Table 6.

Results and discussion

Mass, energy, and carbon flows

Model output provides not only the required amount of scrap and hot metal but also the obtained quantities and compositions of slag and off-gas, which allow to fully represent the mass and energy flows of the BOF process, as represented in Fig. 4. As can be seen, hot metal and steel account for the main part of mass and energy balances.

By contrast, since carbon content of steel is very low, and carbon content in slag is negligible, the major carbon flow is from hot metal and carbon-containing additives to off-gas. Depending on hot metal temperature and strategy, carbon flow varies from 38 to 56 kg/t. The minimum value is obtained for minimum hot metal at 1300 °C using FeSi, while the maximum is reached for maximum hot metal (43 kg/t) with anthracite (13 kg/t).

Influence of hot metal temperature

Direct and indirect CO_2 emissions obtained from model output are plotted in Fig. 5, while total emissions are depicted in Fig. 6. It can be seen the marked effect of hot metal temperature and strategy on BOF carbon footprint since total emissions vary by more than 10%, which means more than 0.15 t of CO_2 per ton of liquid steel, within the considered domain. Although exact emissions can vary from site to site, depending mainly on hot metal temperature and composition but also on processing practices, the obtained results are in good agreement with Ryman and Larsson (2006) who obtained 1.3–1.6 t of CO_2 per ton of liquid steel for common hot metal practices. Moreover, as opposed to previous studies, the obtained results allow BOF engineers to identify or assess local improvements.

The total impact of hot metal temperature can be better appreciated for the neutral strategy in Fig. 6a. As temperature increases, required hot metal to scrap ratio decreases; since direct and indirect emissions are lower for scrap than for hot metal, the total emission diminishes by 0.006 t of CO_2 every 10 °C.

When neutral balance is modified by adding anthracite or iron ore pellets, an increase on CO_2 total emissions of 0.03 and

Table 4 Mass, temperature, and composition of output materials

Material	*m* (t)	*T* (°C)	Chemical composition (% mass)									
			Fe	C	Si	Mn	P	O	N	Ar	CaO	MgO
Steel	300	1700	99.78	0.035	0.001	0.080	0.010	0.090				
Slag	m	m	18.0		m	m	m	m			m	m
Off-gas	m	m		m				m	m	m		

m, model result

Table 5 Indirect CO_2 emissions (t CO_2/t) for input materials from Ryman and Larsson (2006)

H. M.	Scrap	I. O.	Ant.	FeSi	Lime	Dol.	Ar/N_2	O_2
1.1	0.02	0.18	0.05	3.9	1.35	1.35	0.3	0.3

0.05 t, respectively, is observed (Fig. 6c, b). While anthracite increases direct emissions (Fig. 5c), iron ore increases indirect emissions to a greater extent (Fig. 5b). By contrast, the use of FeSi not only saves hot metal but also avoids 0.09 t of CO_2, as shown in Fig. 6d. Despite FeSi higher indirect emissions compared with anthracite, as shown in Table 5, its higher energy contribution together with its null direct emissions makes FeSi the best choice from a carbon footprint perspective.

As can be seen in Fig. 6b, the curve corresponding to maximum hot metal strategy presents a bending point at about 1260 °C. At this point, the maximum iron ore constraint of 2 t is reached. For lower temperatures the amount of hot metal is maximum, and energy can be balanced with a lower iron ore addition. Iron ore does not produce direct emissions and has very low indirect emissions which cause the slightly increasing slope up to 1260 °C. For higher temperatures, energy is balanced by reducing the amount of hot metal and increasing scrap. This causes a remarkable reduction in carbon emissions.

Similarly, the curve corresponding to minimum hot metal with FeSi in Fig. 6d presents a bending point at about 1250 °C. At this point, the maximum scrap constraint of 80 t is reached. For lower temperatures, the amount of FeSi is maximum and energy balance can be met with a lower scrap charge. For higher temperatures, hot metal and scrap are kept almost constant while energy is balanced with a decreasing addition of FeSi, which does not produce direct emissions and has very low indirect emissions, causing the slightly decreasing slope above 1260 °C.

On the contrary, minimum hot metal with anthracite has a uniform slope without bending point, as can be seen in Fig. 6c. Since anthracite has a lower specific energy content than FeSi, the maximum allowed addition of 4000 kg is not enough to balance the maximum scrap load of 80 t even for the maximum considered hot metal temperature of 1300 °C.

Table 6 Process constraints: maximum operating mass (t) of input materials

H. M.	Scrap	I. O.	Ant.	FeSi	Lime	Dol.	Ar/N_2	O_2
280	80	4	4	2	–	–	–	–

Analysis of changes in process design and mitigation measures

The developed model not only provides insights into how hot metal temperature is influencing carbon emissions for typical process conditions but also can be used to analyze the impact of changes in process design. For instance, it is important to analyze which plant constraints should be relaxed in order to further reduce emissions. Figure 7 shows how emissions can be attenuated for minimum hot metal strategy by (a) increasing scrap load capacity from 80 to 84 t; (b) increasing maximum FeSi addition from 2 to 2.2 t; or (c) the combination of both measures. As can be seen, the best option will depend on the plant-specific hot metal temperature distribution but will provide a footprint reduction of more than 0.01 t of CO_2.

Furthermore, the same methodology can also be applied to the assessment of mitigation measures for any plant or production scenario. Here, many options can be envisaged, as (i) the control of thermal losses in hot metal transportation (Niedringhaus et al. 1988; Verdeja et al. 2005); (ii) the use of renewable energy resources for charge preheating (Selvaraj et al. 2016); (iii) the adoption of reducing agents with a lower carbon footprint (Norgate et al. 2012; Mousa et al. 2016); or (iv) the accurate determination of hot metal temperature by models or instruments. This latter possibility has been studied recently, by using both modelling (Díaz et al. 2019) and measurement (Pan et al. 2018) approaches.

The importance of hot metal temperature accuracy resides in the way hot metal is consumed at the BOF. Normally, charge calculation is based on an estimation of hot metal temperature since the real value is not normally known before preparing hot metal load. The model shows that an error of + 10 °C in this estimation requires the addition of 770 kg of anthracite which will cause a net increase on total emission of 0.005 t of CO_2, as depicted in the right side of the emission increase curve in Fig. 8. On the other hand, an error of − 10 °C requires the addition of 320 kg of iron ore, which does not appreciably increase emissions, but the excess of ordered hot metal caused by temperature underestimation will cause a similar increase in CO_2, as can be seen in the left side of the emission increase curve in Fig. 8.

Conclusions

A robust mathematical model has been developed and validated for predicting mass and energy flows in different BOF converters during extended periods of time. The observed daily averaged error in validation tests was less than 1.5% for energy balance and lower than 5% for oxygen balance.

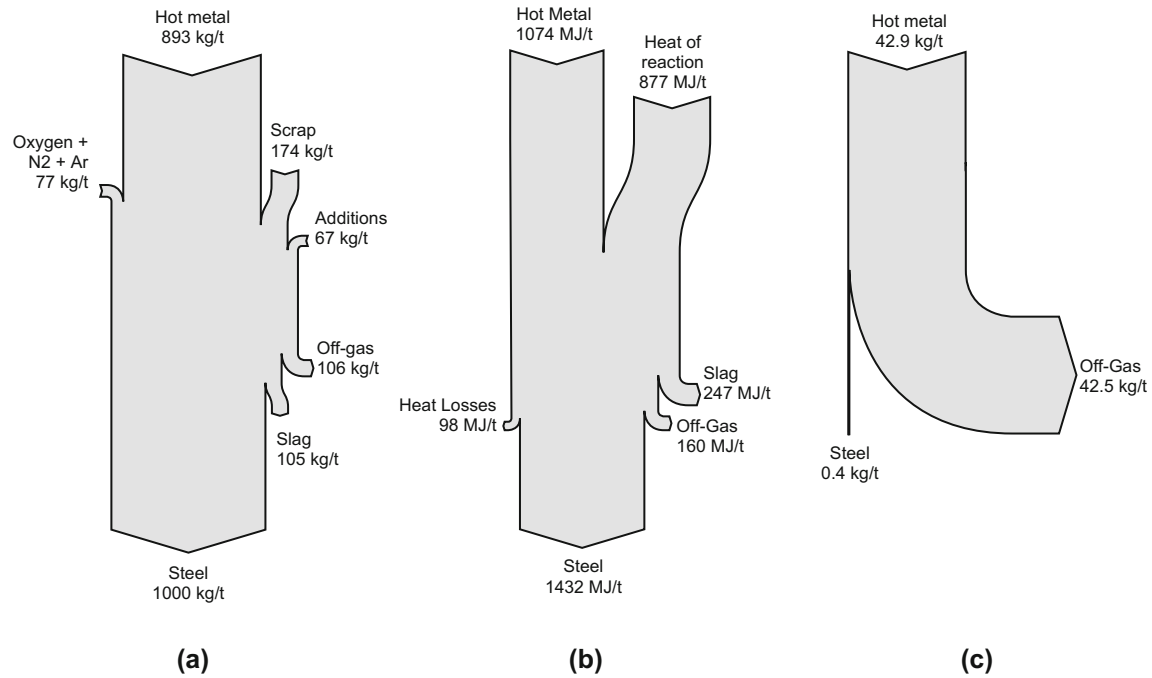

Fig. 4 Sankey diagrams representing **a** mass, **b** energy flows, and **c** carbon, for a heat with neutral hot metal strategy with 1250 °C hot metal temperature

The model has been applied to a wide variable domain, covering minimum, maximum, and neutral hot metal strategies in addition to typical hot metal temperatures, revealing the role of actual process conditions on carbon footprint.

The main carbon flow occurs from hot metal to off-gas and, under the considered process conditions, varies from 38 to 56 kg of carbon per ton of liquid steel. These values correspond to a direct emission between 0.139 and 0.205 tons of CO_2 per ton of liquid steel.

The role of hot metal temperature in combination with hot metal strategy on carbon emissions has been assessed and understood. For neutral strategy, the higher the temperature, the lower the hot metal required and, in consequence, the total CO_2 emission is reduced by 0.006 t every 10 °C of temperature increase. Minimum and maximum strategies always result in an increased carbon footprint of 0.03 to 0.05 t regardless of hot metal temperature, due to the important direct emissions of anthracite and indirect emissions of iron ore, respectively. On the contrary, the use of FeSi instead of anthracite results in much lower emissions, − 0.09 t on average, than for neutral strategy due to its higher energy content together with its null direct emissions.

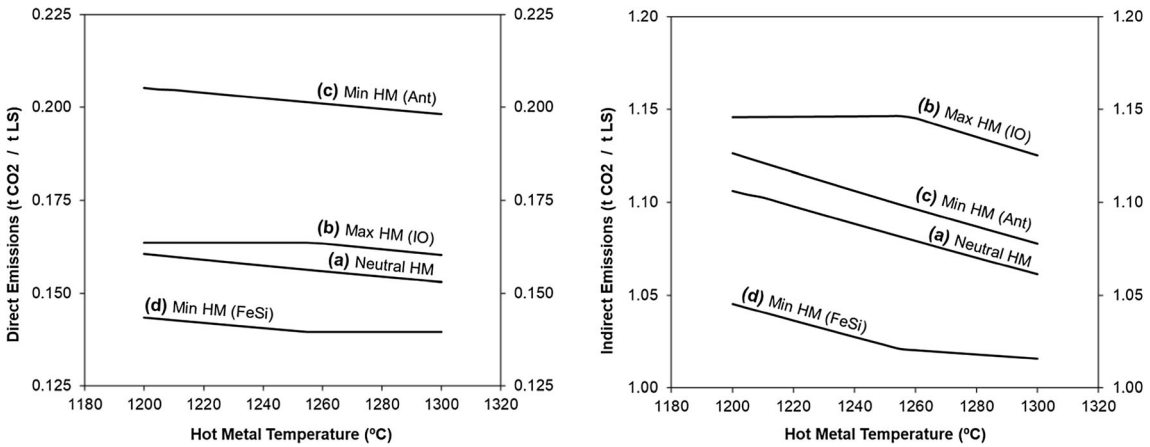

Fig. 5 Calculated direct and indirect CO_2 emissions per ton of liquid steel for different hot metal strategies: (a) neutral energy balance without cooling or heating additives, (b) maximum hot metal with iron ore pellets as coolant, (c) minimum hot metal with anthracite as heating additive, and (d) minimum hot metal with FeSi as heating additive

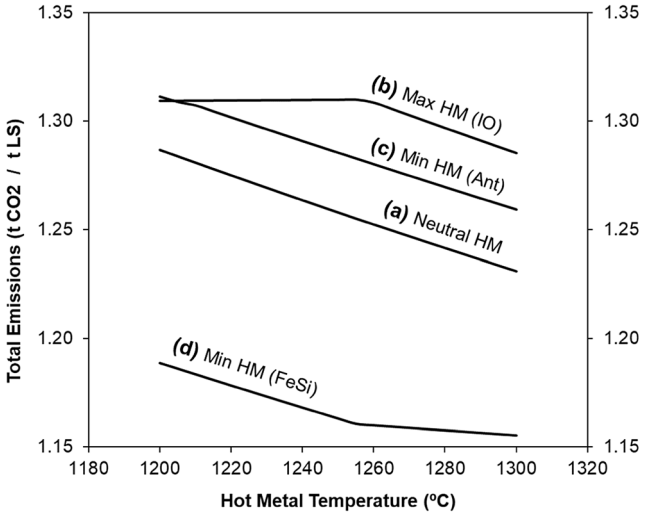

Fig. 6 Calculated total CO_2 emissions per ton of liquid steel for different hot metal strategies: (a) neutral energy balance without cooling or heating additives, (b) maximum hot metal with iron ore pellets as coolant, (c) minimum hot metal with anthracite as heating additive, and (d) minimum hot metal with FeSi as heating additive

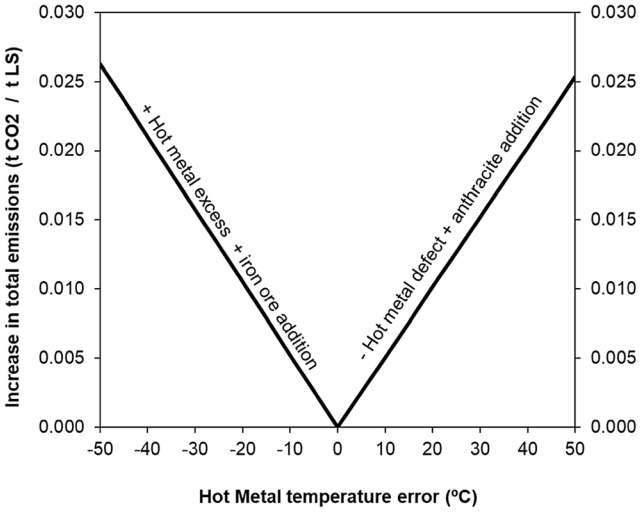

Fig. 8 Effect of hot metal temperature prediction error on total carbon emissions: underestimation of hot metal temperature increases CO_2 mainly for the use of more hot metal, while overestimation requires anthracite which emissions overcome the reduction caused by hot metal consumption reduction

It has been proved that process constraints, in connection with the temperature at which hot metal is received, enormously affect BOF emissions. For instance, a carbon footprint reduction of more than 0.01 t of CO_2 can be simply attained by increasing scrap loading capacity in 4 t or increasing FeSi maximum addition in 200 kg.

The same procedure has been applied to the assessment of improved methods for measuring or predicting hot metal temperature. It was found that a reduction of 10 °C in temperature estimation error allows a net improvement on total CO_2 emission of 0.005 t.

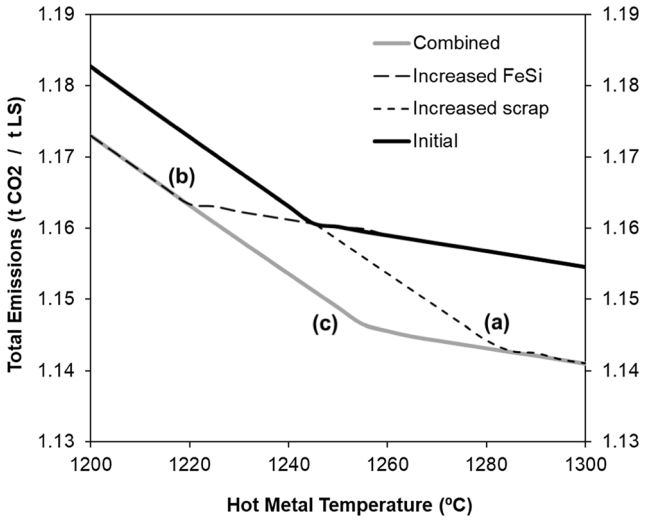

Fig. 7 Expected reduction in total emissions by relaxing initial process constraints: (a) increasing scrap load capacity from 80 to 84 t, (b) increasing maximum FeSi addition from 2 to 2.2 t, and (c) the combination of both measures

It is finally concluded that developments in process and models should be jointly addressed to exploit their full potential for carbon footprint reduction.

Acknowledgments Authors would like to thank ArcelorMittal colleagues for the support and the valuable suggestions they provided. Their environmental commitment has been the best stimulus for this contribution.

References

Ares R, Balante W, Donayo R, Gómez A, Pérez J (2010) Getting more steel from less hot metal at Ternium Siderar steel plant. Rev. Metall. 107:303–308. https://doi.org/10.1051/metal/2010101

Barati M (2010) Energy intensity and greenhouse gases footprint of metallurgical processes: a continuous steelmaking case study. Energy 35(9):3731–3737. https://doi.org/10.1016/j.energy.2010.05.022

Díaz J, Fernandez FJ, Gonzalez A (2018) Prediction of hot metal temperature in a BOF converter using an ANN. International research conference on sustainable energy, engineering, materials and environment, IRCSEEME 2018, 25-27 July, Mieres Spain, pp 27-28

Díaz J, Fernández FJ, Suárez I (2019) Hot Metal Temperature Prediction at Basic-Lined Oxygen Furnace (BOF) Converter Using IR Thermometry and Forecasting Techniques. Energies 12(17): 3235. https://doi.org/10.3390/en12173235

Ghosh A, Chatterjee A (2008) Ironmaking and steelmaking. PHI, New Delhi

Kudrin VA (1985) Steelmaking. MIR, Moscow

Mazumdar D, Evans JW (2010) Elements of mathematical modeling. In: Modeling of steelmaking processes, 1st edn. CRC Press, USA, pp 131–174

Miller TW, Jimenez J, Sharan A, Goldstein DA (1998) Oxygen steelmaking processes. In: Fruehan RJ (ed) The making, shaping, and treating of steel: steelmaking and refining, 11th edn. AISE, Pittsburgh, pp 475–524

Mousa E, Wang C, Riesbeck J, Larsson M (2016) Biomass applications in iron and steel industry: an overview of challenges and opportunities. Renew Sust. Energ. Rev. 65:1247–1266. https://doi.org/10.1016/j.rser.2016.07.061

Niedringhaus JC, Blattner JL, Engel R (1988) ARMCO's experimental 184 mile hot metal shipment. 47 th Ironmaking Conference, 17–20 April, Toronto, Canada, pp 3-7.

Norgate T, Haque N, Sommerville M (2012) Biomass as a source of renewable carbon for iron and steelmaking. ISIJ Int. 52(8):1472–1481. https://doi.org/10.2355/isijinternational.52.1472

Pan D, Jiang Z, Chen Z, Gui W, Xie Y, Yang C (2018) Temperature measurement and compensation method of blast furnace molten iron based on infrared computer vision. IEEE T. Instrum. Meas. 99:1–13. https://doi.org/10.1109/TIM.2018.2880061

Ryman C, Larsson M (2006) Reduction of CO2 emissions from integrated steelmaking by optimised scrap strategies: application of process integration models on the BF–BOF system. ISIJ Int. 46(12):1752–1758. https://doi.org/10.2355/isijinternational.46.1752

Selvaraj J, Harikesavan V, Eshwanth A (2016) A novel application of concentrated solar thermal energy in foundries. Environ. Sci. Poll. R. 23:9312–9322. https://doi.org/10.1007/s11356-015-4996-3

Sickert G, Schramm L (2007) Long-time experiences with implementation, tuning and maintenance of transferable BOF process models. Rev Metall 104:120–127. https://doi.org/10.1051/metal:2007138

Verdeja LF et al (2005) Thermal modelling of a torpedo-car. Rev. Metal. 41:449–455. https://doi.org/10.3989/revmetalm.2005.v41.i6.236

Worldsteel (2018) Steel by topic: life cycle, sustainability, circular economy, and statistics. Worldsteel Association Web. https://www.worldsteel.org/steel-by-topic. Accessed 1 July 2018

Worldsteel (2019) Steel statistical yearbook. Worldsteel Association Web. https://www.worldsteel.org/en/dam/jcr:e5a8eda5-4b46-4892-856b-00908b5ab492/SSY_2018.pdf. Accessed 26 January 2019

Yawata (1986) BOF static and dynamic control models. NSC, Tokyo

Yellishetty M, Mudd GM, Ranjith PG, Tharumarajah A (2011) Environmental life-cycle comparisons of steel production and recycling: sustainability issues, problems and prospects. Environ. Sci. Policy 14:650–663. https://doi.org/10.1016/j.envsci.2011.04.008